

FtsK Initiates the Assembly of a Unique Divisome Complex in the FtsZ-less *Chlamydia trachomatis*


Reviewed Preprint

v1 • December 2, 2024

Not revised

McKenna Harpring, Junghoon Lee, Guangming Zhong, Scot P Ouellette, John V Cox 

Department of Microbiology, Immunology, and Biochemistry. University of Tennessee Health Science Center, Memphis, USA • Department of Pathology, Microbiology, and Immunology, University of Nebraska Medical Center, Omaha, USA • Department of Microbiology, Immunology, and Molecular Genetics, University of Texas Health San Antonio, San Antonio, USA

 https://en.wikipedia.org/wiki/Open_access
 Copyright information

eLife Assessment

In this **important** study, significant advancements are made in how cell division in *Chlamydia trachomatis*, lacking FtsZ, is mediated. With the careful use of fluorescence microscopy and genetic tools, the evidence identifying the DNA translocase, FtsK, as an early and essential component of the divisome, is **convincing**. As this role is distinct from what has been found in most other bacteria, this study will be of broad interest to microbiologists and molecular biologists.

<https://doi.org/10.7554/eLife.104199.1.sa3>

Abstract

Chlamydia trachomatis serovar L2 (Ct), an obligate intracellular bacterium that does not encode FtsZ, divides by a polarized budding process. In the absence of FtsZ, we show that divisome assembly in Ct is initiated by FtsK, a chromosomal translocase. Chlamydial FtsK forms discrete foci at the septum and at the base of the progenitor mother cell, and our data indicate that FtsK foci at the base of the mother cell mark the location of nascent divisome complexes that form at the site where a daughter cell will emerge in the next round of division. The divisome in Ct has a hybrid composition, containing elements of the divisome and elongasome from other bacteria, and FtsK is recruited to nascent divisomes prior to the other chlamydial divisome proteins assayed, including the PBP2 and PBP3 transpeptidases, and MreB and MreC. Knocking down FtsK prevents divisome assembly in Ct and inhibits cell division and septal peptidoglycan synthesis. We further show that MreB does not function like FtsZ and serve as a scaffold for the assembly of the Ct divisome. Rather, MreB is one of the last proteins recruited to the chlamydial divisome, and it is necessary for the formation of septal peptidoglycan rings. Our studies illustrate the critical function of chlamydial FtsK in coordinating divisome assembly and peptidoglycan synthesis in this obligate intracellular bacterial pathogen.

Introduction

Most bacteria divide by a highly conserved process termed binary fission, which occurs through the symmetric division of the parental cell into two daughter cells (Harpring 2023). However, *Chlamydia trachomatis* serovar L2 (Ct), a coccoid, gram-negative, obligate intracellular bacterium divides by a polarized cell division process characterized by an asymmetric expansion of the membrane from one pole of a coccoid cell resulting in the formation of a nascent daughter cell (Abdelrahman 2016 [↗](#); Ouellette SP 2022 [↗](#)).

Ct undergoes a biphasic developmental cycle during infection. Non-replicating and infectious elementary bodies (EBs) bind to and are internalized by target cells. Following internalization, EBs within a membrane vacuole, termed the inclusion, differentiate into replicating reticulate bodies (RBs). After replication, RBs undergo secondary differentiation into EBs, which are released from cells to initiate another round of infection (Abdelrahman 2005 [↗](#)).

In evolving to obligate intracellular dependence, Ct has eliminated several gene products essential for cell division in other bacteria, including the central coordinator of divisome formation, FtsZ (Stephens 1998 [↗](#); Ouellette SP 2020 [↗](#)). This tubulin-like protein forms filaments that associate to form a ring at the division plane (Barrows 2021 [↗](#)), which serves as a scaffold for the assembly of the other components of the bacterial divisome that regulate the processes of septal peptidoglycan (PG) synthesis and chromosomal translocation. Of the twelve divisome proteins shown to be essential for cell division in the model gammaproteobacterial organism, *E. coli*, Ct encodes homologues of FtsK, a chromosomal translocase (Ouellette SP 2012 [↗](#)); FtsQLB, regulators of septal PG synthesis (Ouellette SP 2015 [↗](#); Kaur 2022 [↗](#)), FtsW, a septal transglycosylase (Putman T 2019), and penicillin binding protein 3 (PBP3/FtsI), a septal transpeptidase (Ouellette SP 2012 [↗](#)).

In addition to the divisome, rod-shaped bacteria employ another multiprotein complex, the elongasome, which directs sidewall PG synthesis (Liu 2020 [↗](#)) necessary for cell lengthening and the maintenance of cell shape prior to division. Although Ct is a coccoid organism, it encodes several elongasome proteins, including MreB, MreC, RodA, RodZ, and penicillin binding protein 2 (PBP2), a sidewall transpeptidase (Ouellette SP 2012 [↗](#); Ouellette SP 2014 [↗](#); Cox 2020 [↗](#)). The actin-like protein MreB is essential for cell division (Ouellette SP 2012 [↗](#); Abdelrahman 2016 [↗](#)) and forms septal rings in Ct (Kemege 2015 [↗](#); Liechti 2016 [↗](#); Lee 2020 [↗](#)). These observations led to the proposal that MreB replaces FtsZ in Ct and serves as a scaffold necessary for the assembly of the chlamydial divisome (Lee 2020 [↗](#)).

While inhibitor studies suggest that chlamydial cell division is dependent upon elements of the divisome and elongasome from other organisms (Ouellette SP 2012 [↗](#); Abdelrahman 2016 [↗](#); Cox 2020 [↗](#)), the composition and ordered assembly of the chlamydial divisome and its distribution during polarized budding are undefined. We hypothesized that FtsK, a chromosomal translocase, serves a critical function in regulating the division process of Ct, given previous observations demonstrating it interacts with elements of both the elongasome and divisome (Ouellette SP 2012 [↗](#)). We show here that FtsK initiates the assembly of a hybrid divisome complex in Ct and that MreB does not serve as a scaffold necessary for the assembly of the chlamydial divisome. Rather, chlamydial MreB associates with this hybrid divisome complex late in the chlamydial divisome assembly process, and MreB filament formation is necessary for the formation of septal PG rings. Therefore, our data identify FtsK as the initiator of the cell division process of Ct.

Results

FtsK Forms Foci in *Ct* that Mark the Location of Divisome Complexes

In the *E. coli* linear divisome assembly pathway (Du 2017), FtsK is the first protein downstream of FtsZ encoded by *Ct* (Figure 1A). In other organisms, FtsK is uniformly distributed at the septum of dividing cells (Yu 1998; Wang 2006; Veiga 2017). To investigate the localization of FtsK during cell division in *Ct*, HeLa cells were infected with *Ct*. To overcome the challenges associated with assessing cell morphologies in densely packed inclusions in infected cells, we analyzed FtsK localization in *Ct* derived from lysates of infected HeLa cells at 21 hrs post-infection (hpi) as described previously (Ouellette SP 2022). *Ct* were stained with an antibody against the chlamydial major outer membrane protein (MOMP) and an antibody that recognizes endogenous FtsK. Blotting analysis revealed that this FtsK antibody recognizes a single protein with the predicted molecular mass of FtsK (Supp. Fig. S1A). Our results showed that, unlike FtsK in other organisms, chlamydial FtsK accumulates in discrete foci in the membrane of coccoid cells (Fig. 1B). In cell division intermediates, FtsK localized in foci at the septum, foci at the septum and at the base of the progenitor mother cell, or foci at the base of the progenitor mother cell only (Figure 1C). The chlamydial FtsK foci observed during cell division were not uniformly distributed at the septum, rather septal foci of FtsK were restricted to one side of the MOMP-stained septum. In addition, the FtsK foci were often above or below (marked with arrowheads in Fig. 1C) the MOMP-stained septum. Similar analyses were performed using *Ct* transformed with the pBOMB4-Tet (-GFP) plasmid encoding FtsK with a C-terminal mCherry tag. The expression of this mCherry fusion is under the control of an anhydrotetracycline (aTc)-inducible promoter. HeLa cells were infected with the transformant, and the expression of the fusion was induced by the addition of 10nM aTc to the media of infected cells at 19hpi. RBs were harvested from the induced cells at 21hpi and stained with MOMP antibodies. Imaging analyses revealed that like endogenous FtsK, FtsK-mCherry accumulated in foci in coccoid cells (Fig. 1D), and in division intermediates, it localized in foci at the septum, foci at the septum and at the base of the progenitor mother cell, or foci at the base of the progenitor mother cell only (Fig. 1E). The foci of FtsK-mCherry, like endogenous FtsK, were often offset relative to the plane defined by MOMP staining at the septum (arrowhead in Fig. 1E). Inclusion forming unit (IFU) assays demonstrated that overexpression of the FtsK-mCherry fusion had no effect on chlamydial developmental cycle progression and the production of infectious EBs (Supp. Fig. S2A). While it is possible that the population of FtsK at the base of the mother cell is a remnant of FtsK from a previous division, ~20% of dividing cells have a secondary bud (Fig. 1F), and FtsK and FtsK-mCherry accumulate in foci at the base of secondary buds (arrowheads in Fig. 1G), suggesting that the population of FtsK at the base of the mother cell corresponds to a nascent divisome complex that forms at the site where the daughter cell will arise in the next round of division.

To investigate the distribution of other putative chlamydial divisome components during budding, we transformed *Ct* with plasmids encoding PBP2, PBP3, or MreC with an N-terminal mCherry tag. IFU assays demonstrated that the aTc induced overexpression of the PBP2, PBP3, and MreC fusions had no effect on the developmental cycle progression of *Ct* (Supp. Fig. S2A). In addition, blotting analyses revealed that mCherry antibodies primarily detected single species with the predicted molecular mass of the FtsK, PBP2, PBP3, and MreC fusions in lysates prepared from induced cells (Supp. Fig. S1B). The PBP2, PBP3, and MreC fusions were induced by the addition of 10nM aTc to infected cells at 19hpi, and the induced cells were harvested at 21hpi and stained with MOMP antibodies. Imaging analyses revealed that the PBP2, PBP3, and MreC fusions accumulated in foci in coccoid cells (Fig. 2A), and in cell division intermediates, the fusions accumulated in foci at the septum, in foci at the septum and at the base of the progenitor mother cell, or in foci only at the base of the progenitor mother cell (Fig. 2B). Similar analyses with an MreB_6xHis fusion

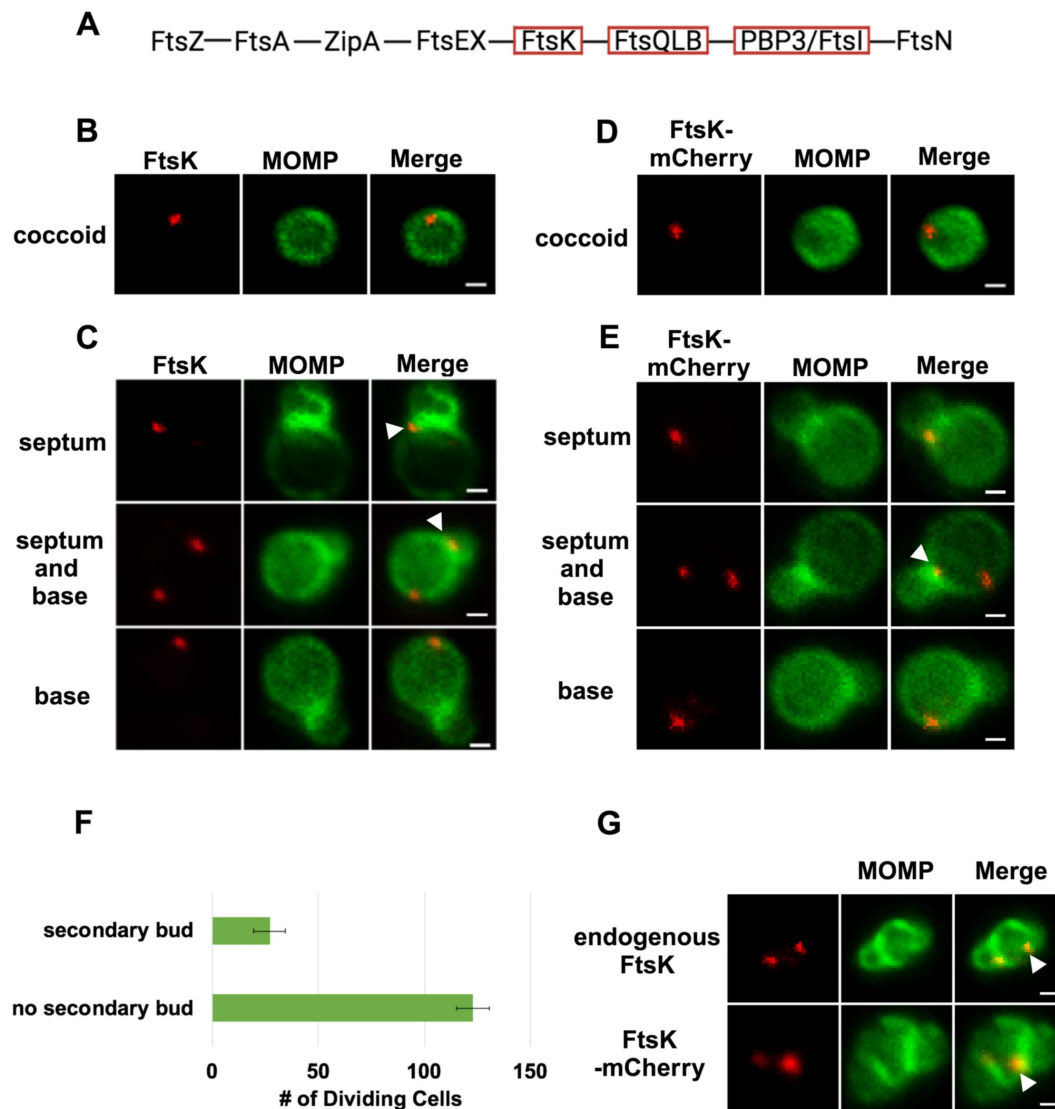


Figure 1

(A) The linear divisome assembly pathway of *E. coli* is shown. *Ct* encodes the divisome proteins boxed in red. HeLa cells were infected with *Ct* L2 and RBs were prepared at 21hpi. The cells were fixed and stained with MOMP (green) and FtsK (red) antibodies. The distribution of FtsK in (B) coccoid cells and in (C) cell division intermediates that had not initiated secondary bud formation is shown. Bars are 1 μ m. HeLa cells were infected with *Ct* transformed with the pBOMB4-Tet (-GFP) plasmid encoding FtsK-mCherry. The fusion was induced with 10nM aTc for 1 hr. and RBs were prepared from infected HeLa cells at 21hpi and stained with MOMP antibodies (green). The distribution of MOMP relative to the mCherry fluorescence (D) in coccoid cells and in (E) cell division intermediates that had not initiated secondary bud formation is shown. Bars are 1 μ m. Arrowheads in C and E denote foci of FtsK above or below the MOMP-stained septum. (F) HeLa cells were infected with *Ct* L2. At 21hpi, the cells were harvested and RBs were stained with MOMP antibodies. The number of dividing cells that had initiated secondary bud formation was quantified in 150 cells. Three independent replicates were performed, and the values shown are the average of the 3 replicates. (G) Endogenous FtsK and FtsK-mCherry accumulate in foci at the septum of secondary buds (marked with arrowheads).

(Lee 2020 [↗](#)) revealed that MreB exhibited a similar localization profile (**Figs. 2A and B** [↗](#)). Each of these fusions, like FtsK, were restricted to one side and were often slightly above or slightly below (marked with arrowheads in **Fig. 2B** [↗](#)) the MOMP-stained septum in dividing cells. The foci of the fusions were also detected at the base of secondary buds (arrowheads in **Supp. Fig. 2B** [↗](#)). Quantification of the localization profiles of endogenous FtsK and the various fusion proteins revealed that the distribution profile of FtsK-mCherry accurately reflected the distribution of endogenous FtsK (**Fig. 2C** [↗](#)). Furthermore, a greater percentage of FtsK was associated with the base of dividing cells (including cells with septum and base, and cells with base alone) suggesting that FtsK associates with nascent divisomes at the base of dividing cells prior to the other putative divisome proteins. Finally, this analysis suggested that MreB associated with nascent divisomes at the base of dividing cells after mCherry-PBP2 and mCherry-PBP3 (marked with # in **Fig. 2C** [↗](#)). The localization profiles of the chlamydial divisome proteins (**Figs. 1** [↗](#) and **2** [↗](#)) likely reflect the assembly of divisome complexes at the septum and at the base of the progenitor mother cell, and the disassembly of the septal divisome when divisome proteins are only present at the base of the mother cell.

Since it was possible that the localization profiles of the mCherry-PBP2 and mCherry-PBP3 fusions were at least in part due to their induced over-expression, we performed similar studies with rabbit antibodies generated against peptides derived from PBP2 or PBP3 (Ouellette SP 2012 [↗](#)). Blotting analyses (**Supp. Fig. S1C** [↗](#)) with these antibodies revealed that they recognized mCherry-PBP2 and mCherry-PBP3 in *Ct* lysates, and immunofluorescent staining with the PBP2 and PBP3-specific antibodies (**Supp. Fig. S1D** [↗](#)) completely overlapped the mCherry fluorescence in cells when the mCherry PBP2 and PBP3 fusions were inducibly expressed in *Ct*. Imaging analyses with the antibodies that recognize endogenous PBP2 and endogenous PBP3 indicated that these antisera detected foci in coccoid cells, and in cell division intermediates, the PBP2 and PBP3 antibodies detected foci at the septum, foci at the septum and at the base of the mother cell, or foci at the base alone (**Supp. Fig. S3A** [↗](#)). Quantification revealed that the localization profiles of endogenous PBP2 and PBP3 in division intermediates (**Supp. Fig. S3B** [↗](#)) were not statistically different than the localization profiles observed for the mCherry fusions of PBP2 and PBP3 (**Fig. 2C** [↗](#)).

The quantification in **Fig. 2C** [↗](#) suggested that FtsK is recruited to nascent divisomes that form at the base of dividing cells prior to the other divisome components. This hypothesis was tested by staining cells expressing the PBP2, PBP3, MreC, or MreB fusions with antibodies that recognize endogenous FtsK. Imaging analyses revealed that in a subset of cells, FtsK was detected in foci at the septum and at the base of dividing cells, while each of the fusions was only detected at the septum where they overlapped the distribution of septal FtsK (**Fig. 2D** [↗](#)), indicating that FtsK is recruited to nascent divisomes at the base of the cell prior to the other divisome components.

MreB Filament Formation is not Required for Foci Formation by FtsK, PBP2, and PBP3

MreB was one of the last components that associated with nascent divisomes forming at the base of the progenitor mother cell (**Fig. 2C** [↗](#)). To investigate whether MreB filament formation was required for the formation of foci by the other chlamydial divisome components, HeLa cells were infected with *Ct* transformed with the FtsK, PBP2, PBP3, MreC, or MreB fusions, and the fusions were induced by adding 10nM aTc to the media of the infected cells at 20hpi for 1hr.

During the induction period, cells were incubated in the absence (**Figs. 3B** [↗](#) and **3D** [↗](#)) or presence (**Figs. 3C** [↗](#) and **3E** [↗](#)) of the MreB inhibitor, A22, which inhibits MreB filament formation (Bean, 2009 [↗](#)). RBs were harvested at 21hpi and stained with the appropriate antibodies to assess the effect of A22 on the cellular distribution of the fusions. As previously shown (Ouellette SP 2012 [↗](#); Cox 2020 [↗](#)), A22 inhibits chlamydial budding and most cells in the population were coccoid following A22 treatment (**Fig. 3A** [↗](#)). Furthermore, approximately 50% of

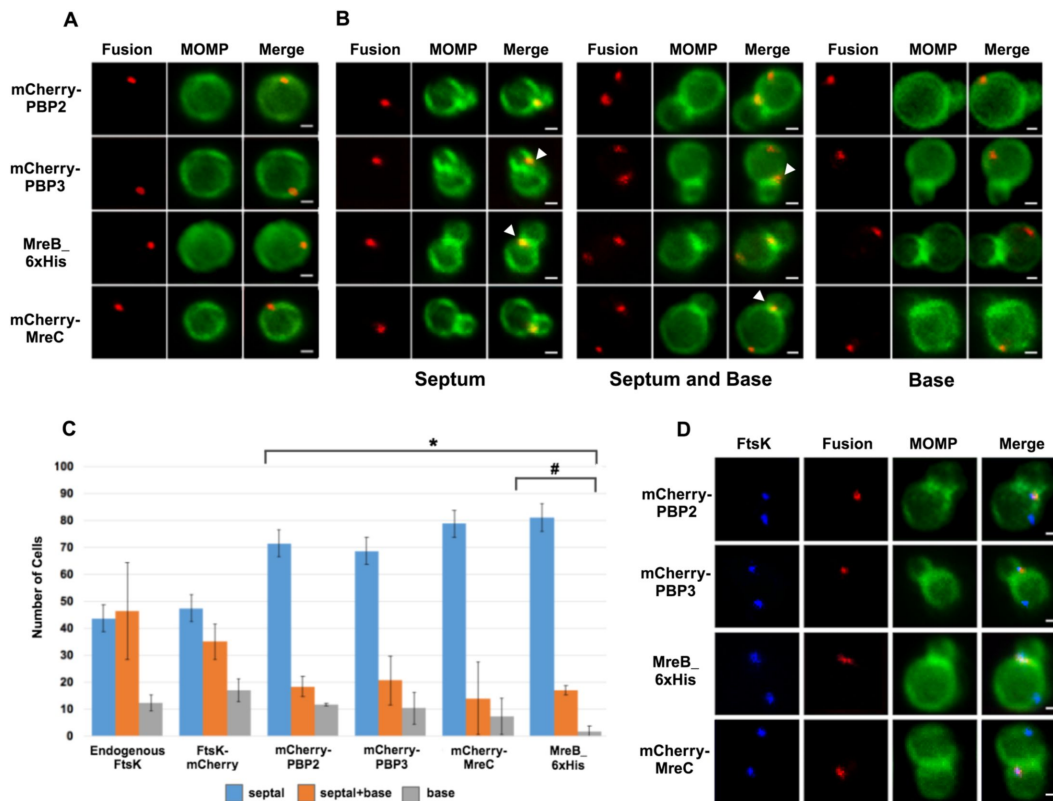


Figure 2

HeLa cells were infected with *Ct* transformed with PBP2, PBP3, or MreC with an N-terminal mCherry tag, or with *Ct* transformed with an MreB_6xHis fusion (Lee 2020). Each of the fusions was induced by adding 10nM aTc to the media at 17hpi. Lysates were prepared at 21hpi and the cells were fixed and stained with a MOMP antibody. The distribution of the mCherry fluorescence in (A) coccooid cells and in (B) dividing cells that had not initiated secondary bud formation is shown. The MreB_6xHis fusion was stained with rabbit anti-6xHis antibody (red) and MOMP antibodies (green). Dividing cells with foci at the septum, foci at the septum and foci at the base of the mother cell, or foci at the base alone are shown for each of the fusions. Arrowheads in B denote foci of the divisome proteins above or below the plane of the MOMP-stained septum. (C) HeLa cells were infected with *Ct* L2 or with *Ct* that inducibly express FtsK-mCherry, mCherry-PBP2, mCherry-PBP3, mCherry-MreC, or MreB_6xHis. The cells were fixed at 21hpi and the distribution of endogenous FtsK, or the mCherry fluorescence in cells inducibly expressing the mCherry fusions, or the distribution of MreB in cells where the MreB_6xHis fusion was inducibly expressed were compared to the distribution of MOMP. The localization profiles were quantified in 100 cells. Three independent replicates were performed, and the values shown are the average of the 3 replicates. Chi-squared analysis revealed that the localization profiles of endogenous FtsK and FtsK-mCherry are not statistically different from each other, but they are statistically different than the PBP2, PBP3, MreC and MreB localization profiles (* - $p < 0.009$). The localization profile of the MreB fusion is also statistically different than the localization profiles of the mCherry fusions of PBP2 and PBP3 (#- $p = 0.05$). (D) HeLa cells were infected with *Ct* transformed with PBP2, PBP3, or MreC with a N-terminal mCherry tag, or with *Ct* transformed with an MreB_6xHis fusion (Lee 2020). The fusions were induced by adding 10 nM aTc to the media at 17hpi. The cells were harvested at 21hpi and *Ct* were harvested and stained with FtsK and MOMP antibodies. The cells expressing the MreB fusion were stained with FtsK, MOMP, and 6xHis antibodies. Imaging analyses revealed that FtsK was present in foci at the septum and in foci at the base in these cells, while each of the fusions was only detected at the septum where they overlapped the distribution of septal FtsK (Bars are 1 μ M).

the untreated control cells were coccoid, which is consistent with prior estimates of the number of non-dividing RBs at this stage of the developmental cycle (Lee 2018 [↗](#)), indicating that our lysis procedure does not lead to a bias in the number of non-dividing coccoid cells in the population. MreB in coccoid cells adopted a diffuse pattern of localization following A22 treatment (Fig 3 [↗](#)). A22 also had a statistically significant effect on the percent of coccoid cells containing MreC foci, but it did not affect the ability of FtsK, PBP2, or PBP3 to form foci in coccoid cells (Figs. 3D [↗](#) and 3E [↗](#)). These data indicate that MreB filaments do not function as a scaffold that is necessary for the assembly of all divisome components in *Ct*.

Effect of *ftsK* and *pbp2* Knockdown on Cell Division and Divisome Assembly in *Ct*

To further investigate the mechanisms that regulate divisome assembly in *Ct*, we inducibly repressed the expression of *ftsK* or *pbp2* using CRISPRi technology, which has been used to inducibly repress the expression of genes in *Ct* (Ouellette SP 2021 [↗](#)). CRISPRi employs a constitutively expressed crRNA that targets an inducible dCas enzyme (dCas12) to specific genes where it binds but fails to cut, thus inhibiting transcription. We transformed *Ct* with the pBOMBL12CRia plasmid that constitutively expresses an *ftsK* or *pbp2*-specific crRNA, which targets sequences in the *ftsK* or *pbp2* promoter regions. To determine whether *ftsK* and *pbp2* transcript levels were altered using this CRISPRi approach, dCas12 expression was induced by the addition of 5nM aTc to the media of infected cells at 8hpi. Control cells were not induced. Nucleic acids were isolated from induced cells and from uninduced control cells at various times, and RT-qPCR was used to measure *ftsK* or *pbp2* transcript levels. This analysis revealed that the induction of dCas12 resulted in ~10-fold reduction in *ftsK* transcript levels by 15hpi in cells expressing the *ftsK*-targeting crRNA (Supp. Fig. S3A [↗](#)), and ~8-fold reduction in *pbp2* transcript levels in cells expressing the *pbp2*-targeting crRNA (Supp. Fig. S3B [↗](#)), while these crRNAs had minimal or no effect on chlamydial *euo* and *omcB* transcript levels, suggesting that the *ftsK* and *pbp2* crRNAs specifically inhibit the transcription of *ftsK* and *pbp2* (Supp. Figs. S3A [↗](#) and S3B [↗](#)). To investigate the effect of *ftsK* or *pbp2* down-regulation on developmental cycle progression, dCas12 was induced by the addition of aTc to the media of infected cells at 4hpi. Control cells were not induced. The cells were then fixed at 24hpi and stained with MOMP and Cas12 antibodies. Imaging analysis revealed that *Ct* morphology was normal and dCas12 was undetectable in the inclusions of uninduced control cells, while foci of dCas12 were observed in the induced cells, and *Ct* in the inclusion exhibited an enlarged aberrant morphology (Supp. Figs. S3C [↗](#) and S3D [↗](#)), suggesting that the inducible knockdown of *ftsK* or *pbp2* blocks chlamydial cell division. In additional studies, we induced dCas12 at 17hpi in cells expressing the *ftsK* or *pbp2*-targeting crRNAs. Lysates were prepared and the cells were fixed at 21hpi, and localization studies revealed that foci of endogenous FtsK and PBP2 were almost undetectable when *ftsK* or *pbp2* were transiently knocked down using this CRISPRi approach (Supp. Fig. S3E [↗](#)).

To assess whether the knockdown of *ftsK* or *pbp2* arrests *Ct* division at a specific stage of polarized budding, HeLa cells were infected with *Ct* transformed with the pBOMBL12CRia plasmids encoding the *ftsK* or *pbp2*-targeting crRNAs. At 17hpi, dCas12 was induced by the addition of 20nM aTc to the media. Control cells were not induced. RBs were harvested from induced and uninduced control cells at 22hpi and stained with MOMP antibodies, and imaging analyses quantified the division intermediates present in the population. These analyses revealed that >60% of the *Ct* in the uninduced controls were at various stages of polarized budding (Figs. 4A and B [↗](#)), while ~90% of the cells were coccoid when *ftsK* was knocked down (Fig. 4A [↗](#)), and ~85% of the cells were coccoid following *pbp2* knockdown (Fig. 4B [↗](#)), suggesting that the initiation of polarized budding of *Ct* is inhibited when *ftsK* or *pbp2* are knocked down.

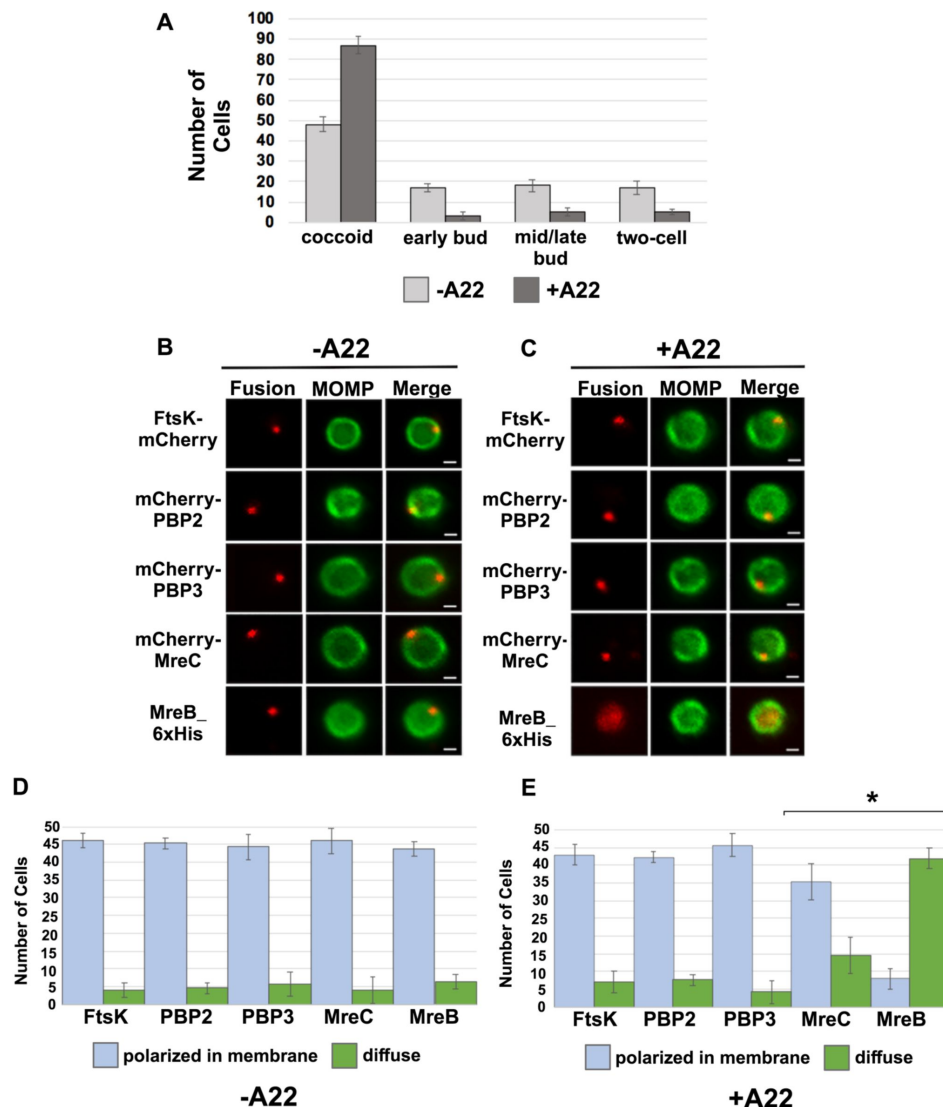


Figure 3

(A) HeLa cells infected with *Ct* L2 were treated with 75 μ M A22 for 1 hour. Control cells were not treated with A22. Lysates were prepared at 21hpi and the number of coccoid and dividing cells in the population were quantified in 100 cells. Three independent replicates were performed, and the values shown are the average of the 3 replicates. (B-E) Alternatively, HeLa cells were infected with *Ct* transformed with plasmids encoding FtsK-mCherry, mCherry-PBP2, mCherry-PBP3, mCherry-MreC, or MreB-6xHis. The fusions were induced at 20hpi with 10nM aTc for 1hr in the absence (B and D) or presence (C and E) of 75 μ M A22. Coccoid cells prepared from the infected cells at 21hpi were stained with MOMP antibodies (green). The MreB-6xHis fusion was also stained with 6xHis antibodies (red). Panel B shows the distribution of the fusions in untreated coccoid cells. Panel C illustrates the effect of A22 on the localization of the fusions in coccoid cells. Bars in B and C are 1 μ m. The distribution of FtsK-mCherry, mCherry-PBP2, mCherry-PBP3, mCherry-MreC, and MreB-6xHis was quantified in (D) control coccoid cells and in (E) A22-treated cells coccoid cells (n=50) is shown. Three replicates were performed, and the values shown in D and E are the averages of the 3 replicates. Student T-test indicated that A22 had a statistically significant effect on the localization of MreB and MreC (* - p<0.01).

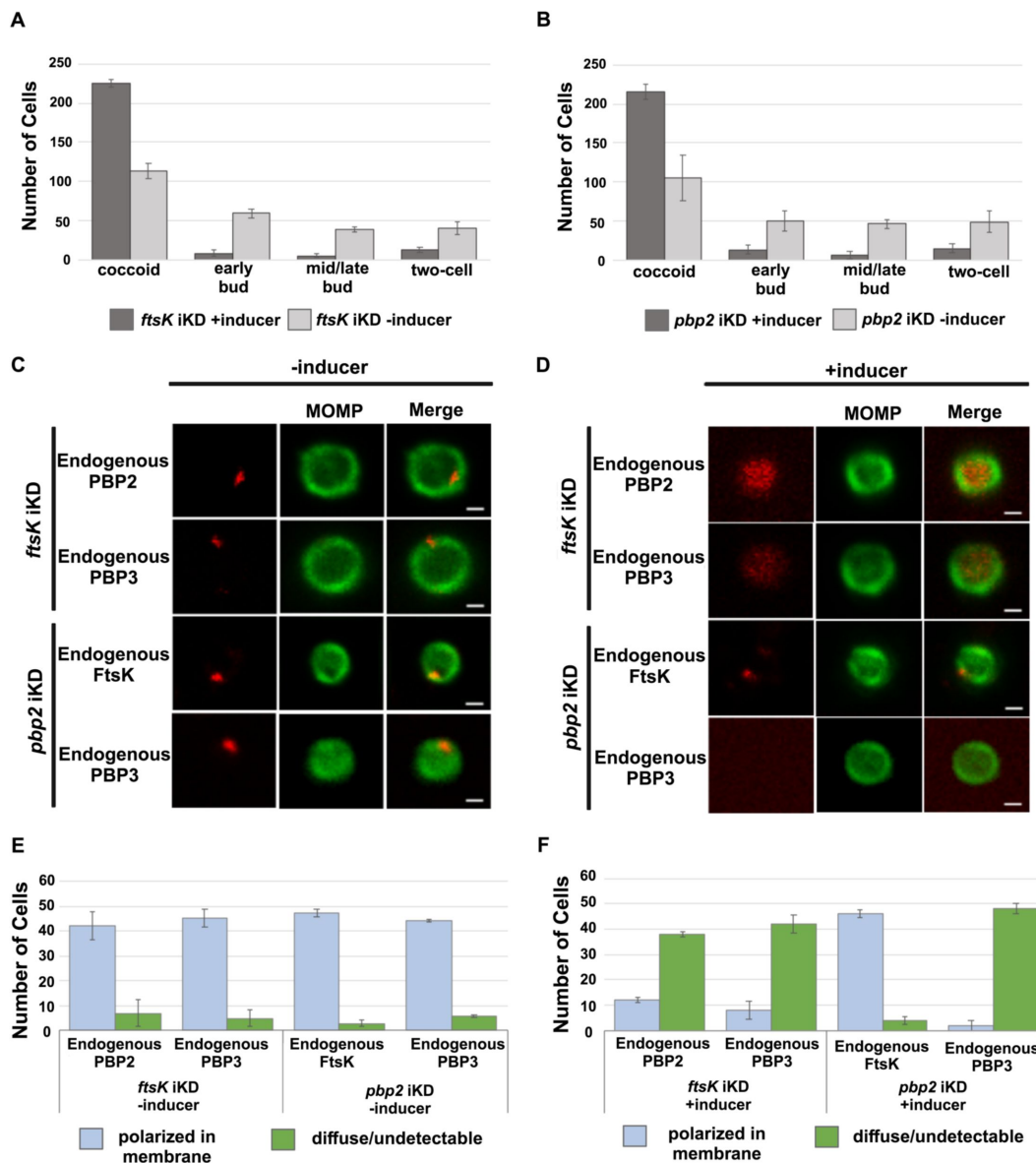


Figure 4

HeLa cells were infected with *Ct* transformed with the pBOMBL-12CRia plasmid, which constitutively expresses a *ftsK* crRNA or *pbp2* crRNA and encodes dCas12 under the control of an aTc-inducible promoter. dCas12 was induced at 17hpi by adding 5nM aTc to the media. In a control infection, the expression of dCas12 was not induced. Cells were harvested at 24hpi and the morphology of *Ct* in induced and uninduced control cells was assessed in 250 cells (A and B). 3 replicates were performed, and the values shown are the averages of the 3 replicates. The localization of endogenous FtsK, endogenous PBP2, and endogenous PBP3 was assessed in cells transformed with the pBOMBL-12CRia plasmid that targets *ftsK* or *pbp2*. The localization is shown in coccoid cells where dCas12 expression was (C) uninduced or (D) induced. White bars are 1µm. The localization profiles of FtsK, PBP2, and PBP3 were quantified in (E) uninduced and (F) induced cells. 3 replicates were performed, and the values shown are the averages of the 3 replicates.

We next examined whether the knockdown of *ftsK* affected foci formation by PBP2 or PBP3 in coccoid cells. HeLa cells were infected with *Ct* transformed with the pBOMBL12CRia plasmid encoding the *ftsK*-targeting crRNA. At 17hpi, dCas12 was induced by the addition of 10nM aTc to the media. Control cells were not induced. RBs were harvested from induced and uninduced control cells at 22hpi, and the localization of endogenous PBP2 and PBP3 in coccoid cells was assessed. This analysis revealed that the number of polarized foci of PBP2 and PBP3 were reduced by approximately 80% in coccoid cells following *ftsK* knockdown (**Fig. 4D** [↗](#)). In similar analyses, we assessed the effect of *pbp2* knockdown on the ability of FtsK and PBP3 to form foci in coccoid cells. While FtsK retained its ability to form foci in coccoid cells following *pbp2* knockdown (**Fig. 4D** [↗](#)), foci of PBP3 were almost entirely absent in *pbp2* knockdown cells (**Fig. 4D** [↗](#)). Quantification of these assays revealed that FtsK is necessary for foci formation by both the PBP2 and PBP3 transpeptidases, while PBP2 is necessary for foci formation by PBP3 (**Figs 4E** [↗](#) and **4F** [↗](#)). Our data place FtsK upstream of, and necessary for, the addition of PBP2 and PBP3 to the *Ct* divisome, and PBP2 upstream of and necessary for the addition of PBP3 to the *Ct* divisome. These results are consistent with inhibitor studies that indicated PBP2 acts upstream of PBP3 in the polarized budding process of *Ct* (Cox 2020 [↗](#)).

To investigate whether the catalytic activity of PBP2 is necessary to maintain its association with the *Ct* divisome, HeLa cells were infected with *Ct*, and mecillinam, an inhibitor of the transpeptidase activity of PBP2 (Kocaoglu 2015 [↗](#); Cox 2020 [↗](#)), was added to the media of infected cells at 20hpi. Cells incubated in the absence of mecillinam were included as a control.

Mecillinam-treated and control cells were harvested at 22hpi and the effect of inhibiting the catalytic activity of PBP2 on the localization of FtsK, PBP2, and PBP3 was determined. As shown previously, mecillinam blocks chlamydial division (Ouellette SP 2012 [↗](#); Cox 2020 [↗](#)), and most cells in the population assumed a coccoid morphology (**Fig. 5A** [↗](#)). We then determined the localization of endogenous FtsK, PBP2, and PBP3 in drug-treated and control coccoid cells.

Mecillinam treatment resulted in a ~50% reduction in the number of cells with polarized foci of PBP2 (**Figs. 5C** [↗](#) and **5E** [↗](#)). There was a similar reduction in polarized foci of PBP3 following mecillinam treatment (**Figs. 5C** [↗](#) and **5E** [↗](#)). These data indicate that the catalytic activity of PBP2 is necessary for PBP2 to efficiently associate with or maintain its association with polarized divisome complexes. Furthermore, consistent with *pbp2* knockdown studies, PBP3 association with the divisome complex is dependent on the prior addition of PBP2 to the complex, but foci formation by FtsK is unaffected when PBP2 foci are reduced in number (**Fig. 5** [↗](#)).

Effect of Inhibitors and *ftsK* Knockdown on PG Organization in *Ct*

To assess the morphology of PG at the septum and the base of dividing cells, we used an EDA-DA labeling strategy (Liechti 2014 [↗](#); Cox 2020 [↗](#)). This approach enabled the detection of PG foci, bars, and rings in dividing *Ct* (Liechti 2021 [↗](#)). Our imaging analysis revealed that PG organization was the same or differed at the septum and at the base of the progenitor mother cell (**Fig. 6A** [↗](#)). In additional analyses, we compared the localization of mCherry-PBP3 to the localization of PG in cells where the expression of this mCherry fusion had been induced by the addition of aTc to the media. This analysis, which was restricted to PG formation at the septum of dividing cells, revealed that multiple foci of PBP3 were associated with a septal PG ring (**Fig. 6B** [↗](#)). Furthermore, the PG ring was at a slight angle relative to the MOMP-stained septum.

Similar analyses revealed that 2 foci of endogenous FtsK were associated with PG that was again at a slight angle to the MOMP-stained septum. This was true even though the PG had not fully reorganized into a ring structure (**Fig. 6B** [↗](#)). To our knowledge, these are the first data in any system to suggest that septal PG synthesis/modification is simultaneously directed by multiple independent divisome complexes.

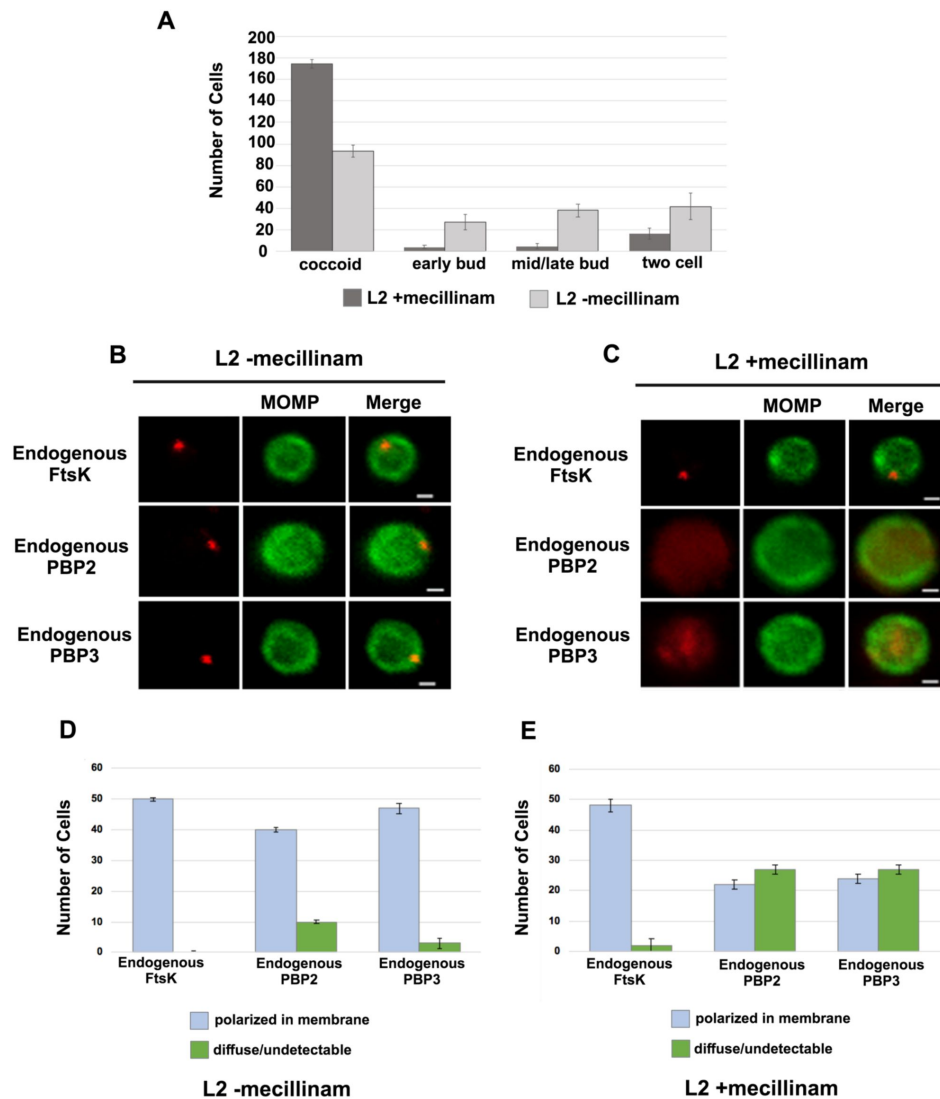


Figure 5

Effect of mecillinam on endogenous FtsK, PBP2, and PBP3 localization. (A) HeLa cells were infected with *Ct* and 20 μ M mecillinam was added to the media at 17hpi. Untreated coccoid cells were included as a control. The cells were harvested at 21hpi and the morphology of MOMP-stained cell was assessed in 200 cells. 3 replicates were performed, and the values shown are the averages of the 3 replicates. (B and C) The localization of endogenous FtsK, endogenous PBP2, and endogenous PBP3 in untreated coccoid or in mecillinam-treated coccoid cells is shown. Bars are 1 μ M. (D and E) Localization of FtsK, PBP2, and PBP3 in untreated and mecillinam-treated coccoid cells was quantified in 50 cells. Three replicates were performed, and the values shown are the averages of the 3 replicates.

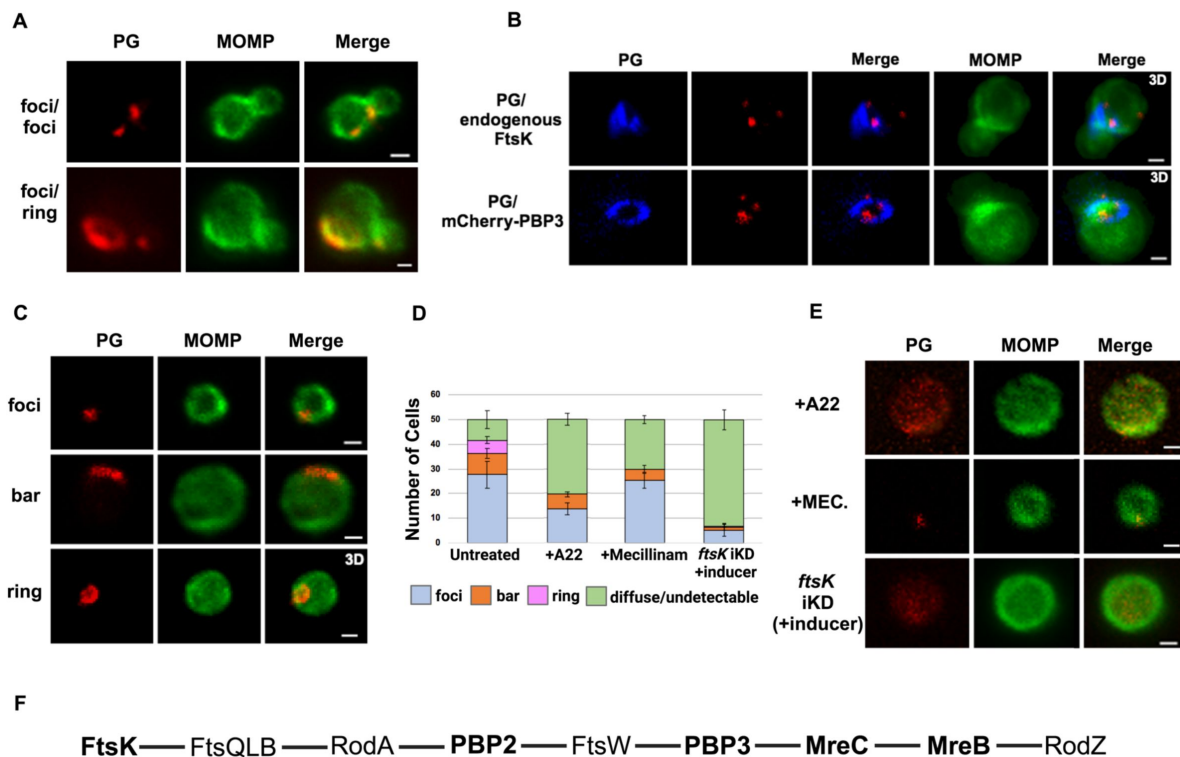


Figure 6

PG distribution in *Ct*. HeLa cells were infected with *Ct* L2. At 17hpi, 4mM ethylene-DA-DA (EDA-DA) was added to the media, the cells were harvested at 21hpi, and the EDA-DA was click labeled and compared to the distribution of MOMP. (A) Imaging revealed that PG organization can vary at the septum and base of dividing cells (B) The localization of click-labeled PG was compared to the localization of endogenous FtsK and mCherry-PBP3 at the septum of dividing cells. 3D projections revealed that multiple foci of each fusion are associated with PG intermediates. (C) PG organization in untreated coccoid cells. (D) Quantification of PG organization in untreated coccoid cells, A22-treated coccoid cells, mecillinam-treated coccoid cells, and in coccoid cells resulting from the inducible knockdown of *ftsK*. Fifty cells were counted for each condition. Three replicates were performed and the average from the 3 replicates is shown. (E) PG organization in A22-treated and mecillinam-treated coccoid cells, and in coccoid cells resulting from the inducible knockdown of *ftsK* is shown. Bars are 1μM. (F) Putative *Ct* divisome assembly pathway in is shown. Proteins characterized in this study are bolded. The ordering of the remaining proteins is based on the assembly of the divisome and elongasome in *E. coli* (Du 2017 [DOI](#); Liu 2020 [DOI](#)).

We then determined the effect of A22 and mecillinam on PG synthesis/morphology. Since both of these drugs induce *Ct* to assume a coccoid morphology, we initially characterized PG organization in untreated coccoid cells. We detected foci, bars, or rings in ~80% of untreated coccoid cells (**Figs. 6C** and **6D**), which make up ~50% of the cells in the inclusion at this stage of the developmental cycle (Lee 2018). Furthermore, each of these PG intermediates exhibited a polarized distribution in untreated coccoid cells (**Fig. 6C**). Although we cannot rule out that continued PG synthesis and reorganization occurs in polarized division intermediates, PG rings can arise prior to any of the morphological changes that occur during the polarized division of *Ct*.

Prior studies have shown that inhibitors of MreB filament formation prevent the appearance of PG-containing structures in *Ct* (Liechti 2014; Ouellette SP 2022). To assess the effect of MreB filament formation on PG synthesis and organization, we infected HeLa cells with *Ct*, and EDA-DA and A22 were added to the media of infected cells at 18hpi. The cells were harvested at 22hpi, lysates were prepared, and PG localization was determined. These analyses revealed that PG was diffuse/undetectable in the majority of A22-treated cells, and, in those cells where PG was still detected, it could not convert into ring structures (**Figs. 6D** and **6E**). In similar experiments, we assessed the effect of mecillinam on the appearance of PG intermediates in coccoid cells. These analyses revealed that PG formed discrete foci or bars in 60% of mecillinam-treated cells (**Figs. 6D** and **6E**). However, these PG intermediates could not convert into PG rings when the transpeptidase activity of PBP2 was inhibited. Finally, we assessed PG organization in cells where *ftsK* was knocked down by inducing dCas12 in the *ftsK* knockdown strain by the addition of aTc to the media of infected cells at 17hpi. Cells were fixed at 21hpi, and localization studies revealed that *ftsK* knockdown had the most dramatic effect on PG localization, which was diffuse/undetectable in ~90% of the cells assayed. Inhibiting divisome assembly by knocking down *ftsK* almost entirely prevented the accumulation of all PG-containing intermediates in *Ct* (**Figs. 6D** and **6E**).

Discussion

The results presented here provide insight into the molecular mechanisms governing the FtsZ-less polarized cell division process of *Ct*. This study is the first to document the ordered assembly of divisome proteins in *Ct* and to investigate the roles of divisome proteins in regulating PG synthesis/organization in this obligate intracellular bacterial pathogen. Based on the results described here, a putative pathway for the assembly of the divisome in *Ct* is shown in **Fig. 6F**.

Our analyses revealed a novel spatiotemporal localization pattern of FtsK during the chlamydial division process. Chlamydial FtsK forms discrete foci at the septum, foci at the septum *and* at the base of the mother cell, or in foci only at the base of the mother cell (**Figure 1**). Our data indicate that the foci at the base of the mother cell correspond to nascent divisome complexes that form prior to the formation of a secondary bud at the base of the progenitor mother cell. Our analyses further revealed there was no correlation between the stage of bud formation by the initial bud (early, mid-late; Ouellette SP 2022), and the appearance of nascent divisomes at the base of the progenitor mother cell (data not shown).

The *Ct* divisome is hybrid in nature, containing elements of the divisome (FtsK and PBP3) and elongasome (PBP2, MreB, and MreC) from other bacteria. Each of these proteins form foci at the septum, foci at the septum and at the base of the mother cell, or foci only at the base of the mother cell, and the foci of each protein are restricted to one side of the MOMP-stained septum (**Figs. 1** and **2**). Knockdown of *ftsK* using CRISPRi revealed that FtsK is necessary for the assembly of this hybrid divisome complex (**Fig. 4**). Knockdown and inhibitor studies further revealed that PBP2 is necessary for the addition of PBP3 to the divisome in *Ct* (**Figs. 4** and **5**).

The chlamydial divisome proteins all form foci in coccoid cells (**Figs. 1** and **2**), and FtsK forms foci in dividing *Ct* that only partially overlap the distribution of PBP2, PBP3, MreC, and MreB (**Fig. 2**). Although it is unclear why FtsK only partially overlaps the distribution of PBP2 and PBP3 in dividing *Ct*, MreB (Liechti 2014; Kemege 2015; Lee 2020) and MreC (**Supp. Fig. S4A**) form rings in dividing cells, and the MreC rings we detected, like PG rings (**Fig. 6**), were at a slight angle relative to the MOMP-stained septum. MreC also forms rings in coccoid cells (**Supp. Fig. S4B**), which may be necessary for PG ring formation in coccoid cells. The relevance of the angled orientation of PG and MreC rings relative to the MOMP-stained septum in division intermediates is unclear. However, it appears to be a conserved feature of the cell division process and may arise because the divisome proteins are often positioned slightly above or below the plane of the MOMP-stained septum (**Figs. 1** and **2**).

Previous studies hypothesized that MreB filaments may substitute for FtsZ and form a scaffold necessary for the assembly of the divisome in *Ct* (Ouellette SP 2012; Ouellette SP 2015; Ouellette SP 2020). However, our analyses have indicated that MreB is one of the last components recruited to nascent divisomes that form at the base of the mother cell in *Ct*, and localization studies revealed that foci formation by FtsK, PBP2, and PBP3 are not dependent on MreB filament formation (**Fig. 3**). Although our data indicate that MreB filaments do not form a scaffold necessary for the assembly of all components of the divisome in *Ct*, MreB filaments are necessary for the conversion of PG foci into PG rings in *Ct* (**Fig. 6**).

FtsZ treadmilling drives its rotational movement at the septum and this may be required for the positioning of peptidoglycan biosynthetic enzymes at the division plane in gram-negative and gram-positive bacteria (Bisson-Filho 2017; Yang 2017). However, to our knowledge, our studies are the first to indicate that multiple independent divisome complexes can simultaneously direct PG synthesis/modification at the septum of a dividing bacterium. The knockdown studies presented here further demonstrated that in the absence of FtsZ, chlamydial FtsK is critical for the initiation of divisome assembly and PG synthesis in *Ct*.

Ct is a member of the Planctomycetes/Verrucomicrobia/Chlamydia superphylum and members of the Chlamydia and Planctomycetes phyla do not encode FtsZ (Rivas-Marín 2016). *Planctospirus limnophila* is a member of the Planctomycetes that divides by polarized budding, and recent knockout studies (Rivas-Marín 2023) indicated that FtsK is the only protein of the chlamydial divisome we characterized here that is essential for the growth of this free-living organism. These results suggest that multiple mechanisms of FtsZ-independent polarized budding have evolved in members of this superphylum. It will be of interest in future studies to determine whether other members of the Planctomycetes that bud (Wiegand 2020) divide using a divisome apparatus similar to *Ct*.

Materials and Methods

Cell Culture

HeLa cells (ATCC, Manassas, VA) were cultured in Dulbecco's Modified Eagle Medium (DMEM; Invitrogen, Waltham, MA) containing 10% fetal bovine serum (FBS, Hyclone, Logan, UT) at 37°C in a humidified chamber with 5% CO₂. HeLa cells were infected with *Ct* serovar L2 434/Bu in the same media. Infections of HeLa cells with chlamydial transformants were performed in DMEM containing 10% FBS and 0.36 U/mL penicillin G (Sigma-Aldrich).

Cloning

The plasmids and primers used for generating mCherry fusions of FtsK, PBP2, PBP3, and MreC are listed in **Supp. Table S1**. The chlamydial *ftsK*, *pbp2*, *pbp3*, and *mreC* genes were amplified by PCR with Phusion DNA polymerase (NEB, Ipswich, MA) using 10 ng *C. trachomatis* serovar L2

genomic DNA as a template. The PCR products were purified using a PCR purification kit (Qiagen) and inserted into the pBOMB4-Tet (-GFP) plasmid, which confers resistance to β -lactam antibiotics. The plasmid was cut at the NotI (FtsK-mCherry) or the KpnI (mCherry-PBP2, mCherry-PBP3, mCherry-MreC) site, and the chlamydial genes were inserted into the cut plasmid using the HiFi DNA Assembly kit (NEB) according to the manufacturer's instructions. The products of the HiFi reaction were transformed into NEB-5 α I^q competent cells (NEB) and transformants were selected by growth on plates containing ampicillin. DNA from individual colonies was isolated using a mini-prep DNA isolation kit (Qiagen), and plasmids were initially characterized by restriction digestion to verify the inserts were the correct size. Clones containing inserts of the correct size were DNA sequenced prior to use.

DNA and RNA purification and RT-qPCR

Total nucleic acids were extracted from HeLa cells infected with *Ct* plated in 6-well dishes as described previously (Ouellette 2015 [\[1\]](#), Ouellette, Blay et al. 2021 [\[2\]](#)). For RNA isolation, cells were rinsed one time with PBS, then lysed with 1mL Trizol (Invitrogen) per well. Total RNA was extracted from the aqueous layer after mixing with 200 μ L per sample of chloroform following the manufacturer's instructions. Total RNA was precipitated with isopropanol and treated with DNase (Ambion) according to the manufacturer's guidelines prior to cDNA synthesis using SuperScript III (Invitrogen). For DNA, infected cells were rinsed one time with PBS, trypsinized and pelleted before resuspending each pellet in 500 μ L of PBS. Each sample was split in half, and genomic DNA was isolated from each duplicate sample using the DNeasy extraction kit (Qiagen) according to the manufacturer's guidelines. Quantitative PCR was used to measure *C. trachomatis* genomic DNA (gDNA) levels using an *euo* primer set. 150ng of each sample was used in 25 μ L reactions using standard amplification cycles on a QuantStudio3 thermal cycler (Applied Biosystems) followed by a melting curve analysis. *ftsK*, *pbp2*, *euo*, and *omcB* transcript levels were determined by RT-qPCR using SYBR Green as described previously (Ouellette SP 2021 [\[3\]](#)) (see **Supp. Table S2** [\[4\]](#) for primers used for measuring gDNA levels and RT-qPCR). Transcript levels were normalized to genomes and expressed as ng cDNA/gDNA.

Transformation of *Ct*

Ct was transformed as described previously (Wang 2011 [\[5\]](#)). Briefly, HeLa cells were plated in a 10cm plate at a density of 5×10^6 cells the day before beginning the transformation procedure. *Ct* lacking its endogenous plasmid (-pL2) was incubated with 10 μ g of plasmid DNA in Tris-CaCl₂ buffer (10 mM Tris-Cl pH 7.5, 50 mM CaCl₂) for 30 min at room temperature.

HeLa cells were trypsinized, washed with 8mL of 1x DPBS (Gibco), and pelleted. The pellet was resuspended in 300 μ L of the Tris-CaCl₂ buffer. *Ct* was mixed with the HeLa cells and incubated at room temperature for an additional 20 min. The mixture was added to 10mL of DMEM containing 10% FBS and 10 μ g/mL gentamicin and transferred to a 10cm plate. At 48hpi, the HeLa cells were harvested and *Ct* in the population were used to infect a new HeLa cell monolayer in media containing 0.36 U/ml of penicillin G to select for transformants. The plate was incubated at 37°C for 48 hours. These harvest and re-infection steps were repeated every 48hrs until inclusions were observed.

Immunofluorescence Microscopy

HeLa cells were seeded in 10cm plates at a density of 5×10^6 cells per well the day before the infection. *Ct* L2 or chlamydial strains transformed with plasmids encoding FtsK-mCherry, mCherry-PBP2, mCherry-PBP3, or mCherry-MreC or with plasmids that direct the constitutive expression of the crRNAs targeting the *pbp2* or *ftsK* promoters were used to infect HeLa cells in DMEM. For experiments with the transformants, aTc was added to the media of infected cells at the indicated concentration and time. At 21hpi, cells were detached from the 10cm plate by scraping and pelleted by centrifugation for 30 seconds. The pellet was resuspended in 1 mL of 0.1x

PBS (Gibco) and transferred to a 2mL tube containing 0.5mm glass beads (ThermoFisher Scientific). Cells were vortexed for 3 mins. then centrifuged at 800rpm for 2 mins. in a microfuge. 20μLs of the supernatant was mixed with 20μLs of 2x fixing solution (6.4% formaldehyde and 0.044% glutaraldehyde) and incubated on a glass slide for 10 min at room temperature. Cells were washed with 3 times with PBS, and the cells were permeabilized by incubation with PBS containing 0.1% Triton X-100 for 1 min. Cells were washed with PBS two times. For experiments with Ct L2, the cells were incubated with a goat primary antibody against the major outer-membrane protein (MOMP; Meridian, Memphis, TN), and the mouse primary antibody that recognizes endogenous FtsK raised against recombinant CT739 protein (<https://doi.org/10.1099/mic.0.047746-0>), or with rabbit antibodies raised against peptides derived from PBP 2 or PBP3 (Ouellette SP 2012). Briefly, chlamydial antigens or peptides emulsified with Freund's incomplete adjuvant were used to immunize animals via intramuscular injections three times with an interval of 2 weeks. Antisera were collected from the immunized animals 2 to 4 weeks after the final immunization as the primary antibodies. After the primary antibody labeling, the cells were then rinsed with PBS and incubated with donkey anti-goat IgG (Alexa 488) and donkey anti-mouse IgG (Alexa 594) or donkey-anti-rabbit IgG (Alexa 594) secondary antibodies (Invitrogen). Experiments in which we visualized the distribution of the various mCherry fusions, the localization of the mCherry fluorescence was compared to the distribution of MOMP. In some experiments, we determined the distribution of the MreB_6x His fusion by staining cells expressing the fusion with a rabbit anti-6x His antibody (Abcam, Cambridge, MA) and the goat anti-MOMP antibody followed by the appropriate secondary antibodies. Cells were imaged using Zeiss AxioImager2 microscope equipped with a 100x oil immersion PlanApochromat objective and a CCD camera. During image acquisition, 0.3μm xy-slices were collected that extended above and below the cell. The images were collected such that the brightest spot in the image was saturated. The images were deconvolved using the nearest neighbor algorithm in the Zeiss Axiovision 4.7 software. Deconvolved images were viewed and assembled using Zeiss Zen-Blue software. For each experiment, three independent replicates were performed, and the values shown for localization are the average of the 3 experiments. In some instances, 3D projections of the acquired xy slices were generated using the Zeiss Zen-Blue software.

Peptidoglycan (PG) labeling

PG was labeled by incubating cells with 4mM ethylene-D-alanine-D-alanine (E-DA-DA) as described (Cox 2020). The incorporated E-DA-DA was fluorescently labeled using the Click & Go™ labeling kit (Vector Laboratories). The distribution of fluorescently labeled PG was compared to the distribution of MOMP or the distribution of the various mCherry fusions. Three independent replicates were performed, and the values shown are the average of the 3 experiments.

Inclusion forming unit assay

HeLa cells were infected with Ct (-pL2) transformed with the pBOMB4 Tet (-GFP) plasmid encoding the indicated aTc-inducible gene. At 8hpi, aTc was added to the culture media at the indicated concentration. Control cells were not induced. At 48hpi, the HeLa cells were dislodged from the culture dishes by scraping and collected by centrifugation. The pellet was resuspended in 1 mL of 0.1x PBS (Gibco) and transferred to a 2mL tube containing 0.5mm glass bead tubes (ThermoFisher Scientific). Cells were vortexed for 3 min. followed by centrifugation at 800rpm for 2 min. The supernatants were mixed with an equal volume of a 2x sucrose-phosphate (2SP) solution (ref) and frozen at -80°C. At the time of the secondary infection, the chlamydiae were thawed on ice and vortexed. Cell debris was pelleted by centrifugation for 5 min at 1k x g at 4°C. The EBs in the resulting supernatant were serially diluted and used to infect a monolayer of HeLa cells in a 24-well plate. The secondary infections were allowed to grow at 37°C for 24 hrs before they were fixed and labeled for immunofluorescence microscopy by incubating with a goat anti-MOMP antibody followed by a secondary donkey anti-goat antibody (Alexa Fluor 594). The cells were rinsed in PBS and inclusions were imaged using an EVOS imaging system (Invitrogen). The number of inclusions were counted in 5 fields of view and averaged. Three independent replicates

were performed, and the values from the replicates were averaged to determine the number of inclusion forming units. Chi-squared analysis was used to compare IFUs in induced and uninduced samples.

Effect of A22 and mecillinam on the profile of division intermediates and on PG and divisome protein localization in *Ct*

HeLa cells were infected with *Ct* transformed with the pBOMB4-Tet (-GFP) plasmid encoding FtsK-mCherry, mCherry-PBP2, mCherry-PBP3, mCherry-MreC, or MreB-6xHis. The fusions were induced at 20hpi with 10nM aTc for 1hr in the absence or presence of 75 μ M A22. At 22hpi, cells were harvested and prepared for staining as described above. Three independent replicates were performed, and the values shown for localization are the average of the 3 experiments.

HeLa cells were infected with *Ct* L2 and 20 μ M mecillinam (Sigma) was added to the media of infected cells at 17 hpi. Control cells were untreated. At 22 hpi, infected cells were harvested and RBs were prepared and stained with MOMP, FtsK, PBP2 or PBP3 antibodies as described above. Alternatively, cells were incubated with 4mM EDA-DA at 17hpi in the presence or absence of 20 μ M mecillinam. The cells were harvested at 22hpi, and RBs were prepared and PG was click-labeled, and its distribution was visualized in MOMP-stained cells as described above. Three independent replicates were performed, and the values shown for localization are the average of the 3 experiments.

Immunoblotting

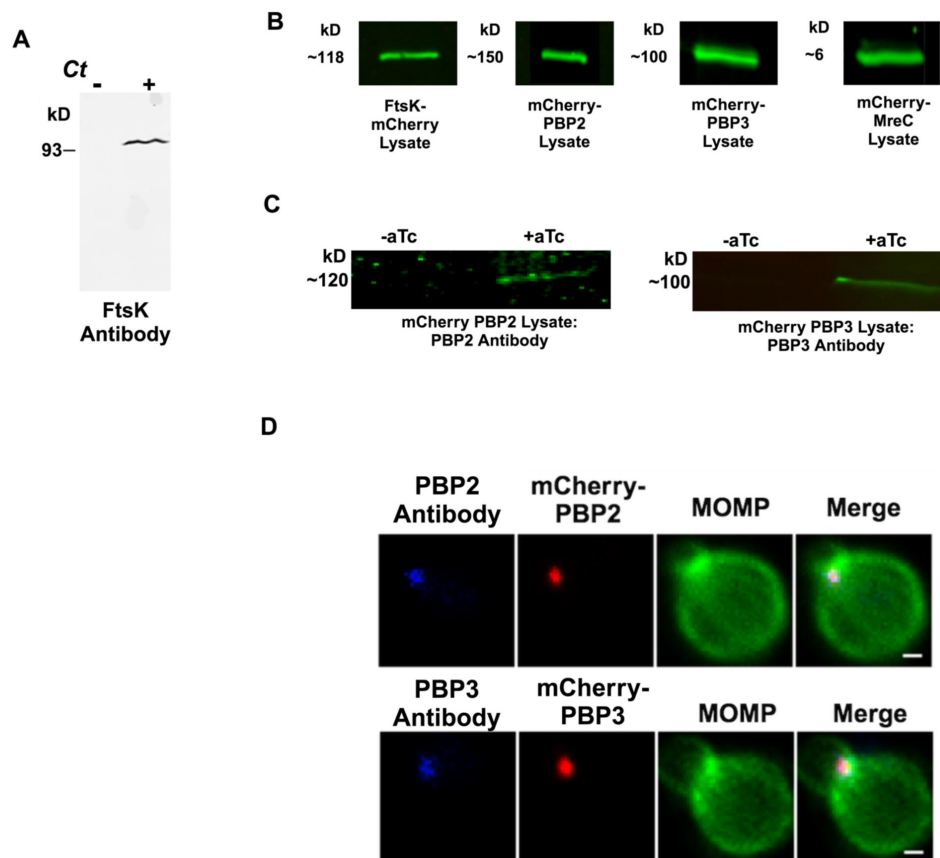
HeLa cells infected with *Ct* L2 were harvested by scraping the infected cells from the plate at 24hpi. Uninfected HeLa cells were included as a control. The HeLa cells were pelleted by centrifugation, resuspended in SDS sample buffer and electrophoresed on a 10% SDS polyacrylamide gel. The gel was electrophoretically transferred to nitrocellulose (Schleicher and Schuell), and the filter was incubated with mouse polyclonal antibodies raised against chlamydial FtsK. The filter was rinsed and incubated with 800 donkey anti-mouse IgG secondary antibodies (LICOR, Lincoln, NE) and imaged using a LICOR Odyssey imaging system.

HeLa cells were infected with *Ct* transformed with plasmids that inducibly express FtsK-mCherry, mCherry-PBP2, mCherry-PBP3, or mCherry-MreC. The fusions were induced by the addition of 10nM aTc to the media of infected cells at 17hpi. The cells were harvested and pelleted at 21hpi. The cell pellet was resuspended in 1 mL of 0.1x PBS (Gibco) and transferred to a 2mL tube containing 0.5mm glass beads (ThermoFisher Scientific). Cells were vortexed for 3 min. followed by centrifugation at 800rpm for 2 min. The supernatant was collected and centrifuged for 3 min at 13,000 rpm and the pellet containing *Ct* was resuspended in TBS containing 1% TX-100, 1X protease inhibitor cocktail (Sigma), and 5 μ M lactacystin. The suspension was sonicated 3 times on ice and centrifuged at 13,000 rpm for 3 mins. The supernatant was collected and mixed with SDS sample buffer. The samples were boiled and electrophoresed on a 10% SDS polyacrylamide gel, and the gel was electrophoretically transferred to nitrocellulose. The blots from these analyses were probed with a rabbit anti-mCherry primary antibody (Invitrogen) and a 800 donkey anti-rabbit IgG secondary antibodies (LICOR, Lincoln, NE). The filters were imaged using a LICOR Odyssey imaging system.

HeLa cells were infected with *Ct* transformed with the pBOMB4-Tet (-GFP) plasmid encoding mCherry-PBP2 or mCherry-PBP3. The fusions were induced with 10nM aTc at 17hpi. Uninduced cells were included as a control. The cells were harvested at 21hpi, and samples were processed for immunoblotting as described above. The blots were probed with rabbit polyclonal antibodies raised against peptides derived from chlamydial PBP2 or PBP3 (Quellette SP 2012 [\[4\]](#)). The blots were then rinsed and incubated with 800 donkey anti-rabbit IgG secondary antibodies (LICOR, Lincoln, NE). The filters were imaged using a LICOR Odyssey imaging system.

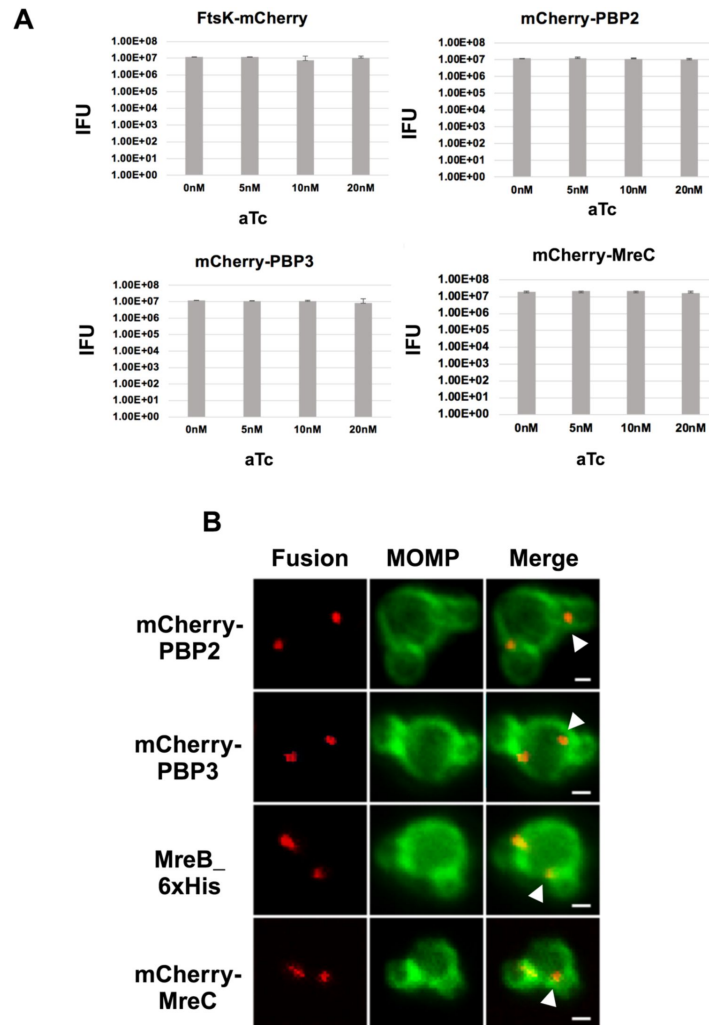
Acknowledgements

We thank Dr. H. Caldwell (NIH/NIAID) for providing eukaryotic cell lines and Dr. I. Clarke (University of Southampton) for providing the plasmidless strain of *C. trachomatis* serovar L2. Funding for this work was supported in part by the National Institutes of Health (NIH/NIGMS) grant R35GM151971 to SPO and by the NSF grant 1817578 to JVC.



Supp. Fig. S1

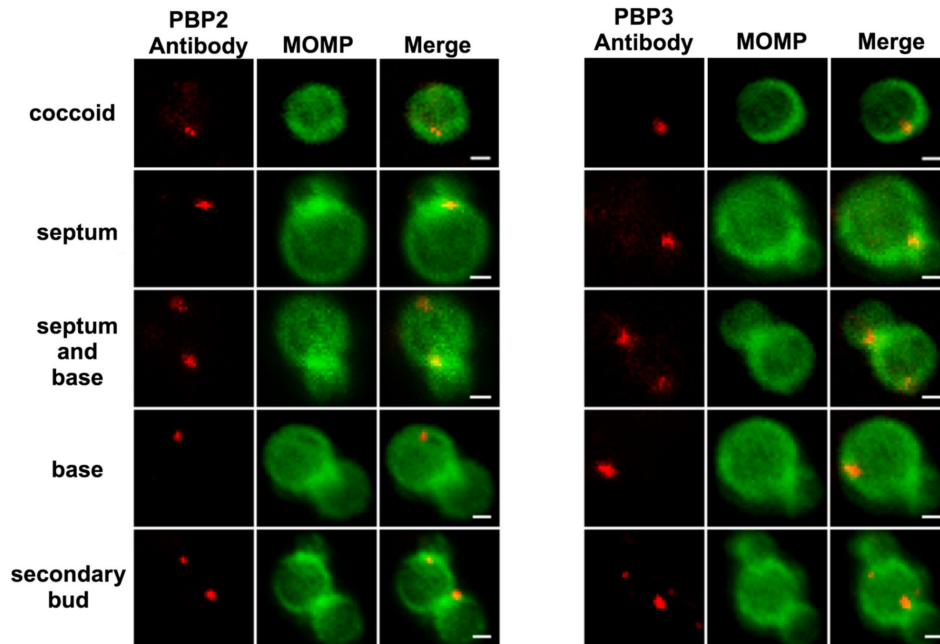
(A) Lysates were prepared from uninfected HeLa cells and HeLa cells infected with *Ct* L2. At 21hpi, lysates were prepared and characterized by immunoblotting with FtsK-specific antibodies. (B) HeLa cells were infected with *Ct* transformed with mCherry fusions of FtsK, PBP2, PBP3, or MreC. The fusions were induced with 10nM aTc at 17hpi. HeLa cells were harvested at 21hpi and lysates were prepared and characterized by immunoblotting analysis with a rabbit polyclonal mCherry antibodies. (C) HeLa cells were infected with *Ct* transformed N-terminal fusions of PBP2 or PBP3. The fusions were induced (+aTc) at 17hpi. Controls were not induced (-aTc). The cells were harvested at 21hpi and lysates were prepared as described in the Methods and characterized by immunoblotting analysis with rabbit antibodies raised against peptides derived from chlamydial PBP2 or PBP3. The PBP3 antibody primarily detects a single species with the predicted molecular mass of mCherry-PBP3 in the induced sample, The PBP2 antibody primarily detects a single species of 120kD in the induced sample, which is smaller than the predicted molecular mass of mCherry-PBP2 (~150kD). The failure to detect full length mCherry-PBP2 may be due to the masking of the epitope recognized by the PBP2 antibody by the N-terminal mCherry tag in the full-length protein. (D) HeLa cells were infected with *Ct* transformed with mCherry-PBP2 or mCherry-PBP3. The fusions were induced by the addition of 10nM aTc to the media of the infected cells at 19hpi. Infected cells were harvested at 21hpi and lysates were prepared and stained with the PBP2 or PBP3 antibodies. The staining with the PBP2 and PBP3 antibodies completely overlaps the mCherry fluorescence from the mCherry-PBP2 and mCherry-PBP3 fusions (Bars are 3μM)



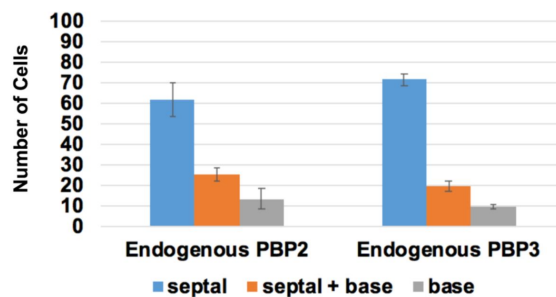
Supp. Fig. S2

(A) HeLa cells were infected with *Ct* transformed with FtsK-mCherry, mCherry-PBP2, mCherry-PBP3, and mCherry-MreC. The fusions were uninduced or induced by the addition of varying amounts of aTc to the media of the infected cells at 8hpi. The cells were harvested at 48hpi and *Ct* were isolated. The number of infectious *Ct* in the lysates was measured by an IFU assay. Chi-squared analysis revealed that induction of the fusions did not have a statistically significant effect on the growth of *Ct* and the production of infectious EBs. (B) Each of the mCherry fusions accumulate in foci at the septum and in foci at the base (marked with arrowheads) of dividing cells with secondary buds.

A

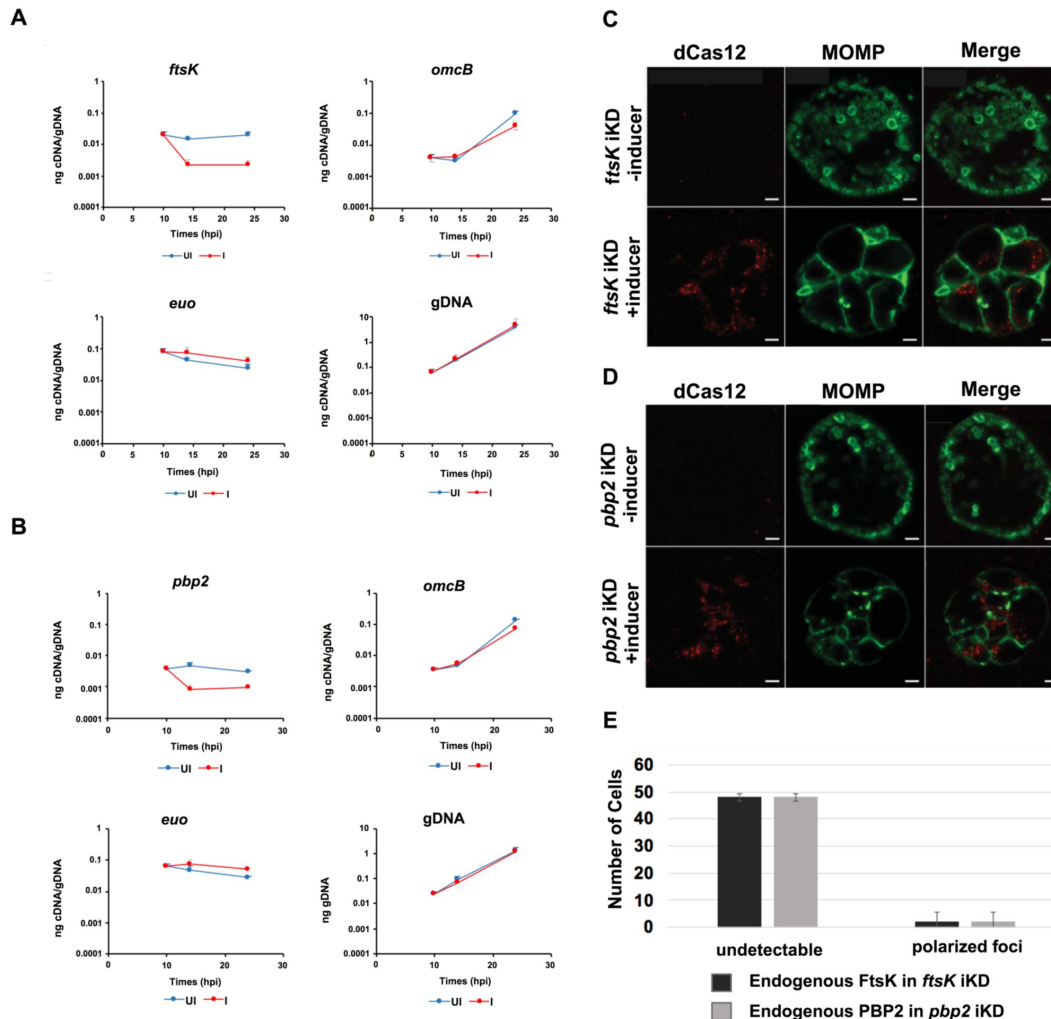


B



Supp. Fig. S3

(A) Localization analyses with rabbit polyclonal antibodies that recognize endogenous PBP2 or PBP3. These analyses revealed that endogenous PBP2 and PBP3 accumulate in foci in coccoid cells, and in foci at the septum, foci at the septum and base, or in foci at the base alone in cell division intermediates in *Ct*. PBP2 and PBP3 foci are also detected at the base of secondary buds. Bars are 1 μ m (B) Quantification revealed that the localization profiles of endogenous PBP2 and PBP3 were not statistically different than the localization profiles of the mCherry-PBP2 and mCherry-PBP3 fusions shown in Fig. 2C.

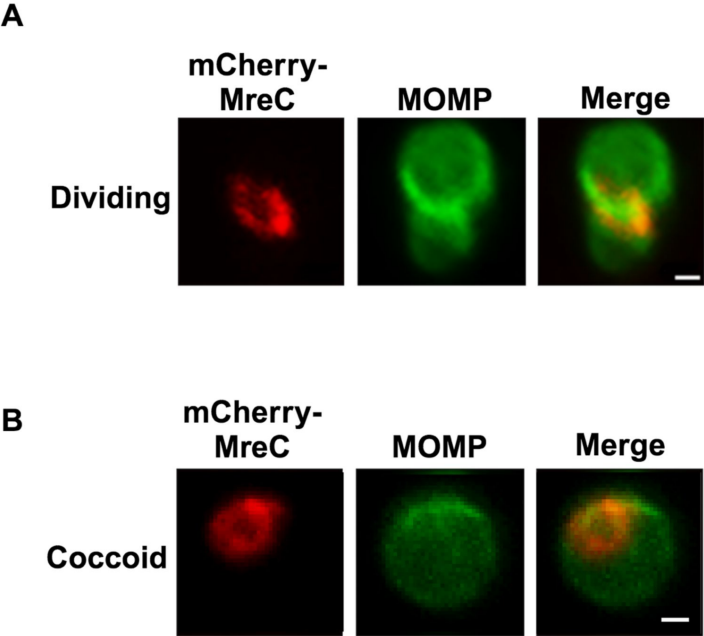


Supp. Fig. S4

HeLa cells were infected with Ct transformed with the pBOMBL12CRia plasmid that constitutively expresses *ftsK* or *pbp2*-targeting crRNAs. dCas12 expression was induced by the addition of 5nM aTc to the media of infected cells at 8hpi. Control cells were not induced. Nucleic acids were isolated from induced cells and from uninduced controls at various times post-infection, and RT-qPCR was used to measure *ftsK* or *pbp2* transcript levels. (A) The induction of dCas12 resulted in ~10-fold reduction in *ftsK* transcript levels in cells expressing the *ftsK*-targeting crRNA, (B) and ~8-fold reduction in *pbp2* transcript levels in cells expressing the *pbp2*-targeting crRNA, while these crRNAs had minimal or no effect on chlamydial *euo* and *omcB* transcript levels. HeLa cells were infected with Ct transformed pBOMBL12CRia plasmid that constitutively expresses a (C) *ftsK* or (D) *pbp2*-targeting crRNA. dCas12 expression was induced by the addition of 5nM aTc to the media of infected cells at 8hpi. Control cells were not induced. The infected cells were fixed at 24hpi and stained with MOMP and Cas12 antibodies. Ct morphology was normal and dCas12 was undetectable in the inclusions of uninduced control cells. Foci of dCas12 were observed in induced cells, and Ct in the inclusion exhibited an enlarged aberrant morphology. Bars in C and D are 2 μm. (E) HeLa cells were infected with Ct transformed with the pBOMBL12CRia plasmid that constitutively expresses a *ftsK* or *pbp2*-targeting crRNA. dCas12 was induced at 17hpi by the addition of 10nM aTc to the media. Control cells were not induced. The cells were harvested at 21hpi, and Ct were prepared and stained with antibodies that recognize that endogenous FtsK or PBP2. Quantification shows that polarized foci of FtsK and PBP2 were almost undetectable when *ftsK* or *pbp2* were transiently knocked down.

Supp. Fig. S5

MreC rings in (A) dividing *Ct* and in (B) coccoid *Ct*.



Supp. Table S1

List of primers and plasmids used for cloning mCherry fusions of FtsK, PBP2, PBP3, MreB and MreC.

Primer Name	Primer Sequence (5'-3')	GC content (%)	TM (°C)
FtsK_mCherry (fwd)	AGAGGAGAAAGGATCTGCGGCCGCATGGGAAAAGAACGGAAGAAAGCAAG	52	72.8
FtsK_mCherry (rvs)	CCCTTAGAGACCATTGCGGCCGCATCGTCCTGATTTGATAATTGGACTAGTATTTGAC	47	72.4
mCherry_PBP2 (fwd)	ATGGTCTCTAAGGGCGAGGAAGAC	54	59.1
mCherry_PBP2 (rvs)	ATGGTCGACCGGTACCCTAGCTGAAAGATTTTTACGAATCTCTTCCCATTCTCTATC	41	70.2
mCherry_PBP3 (fwd)	ATGGTCTCTAAGGGCGAGGAAGAC	54	59.1
mCherry_PBP3 (rvs)	ATGGTCGACCGGTACCCTATTTGCGATTCCATTCTCATATAGCAG	48	69.9
mCherry_MreC (fwd)	ATGGTCTCTAAGGGCGAGGAAGAC	54	59.1
mCherry_MreC (rvs)	ATGGTCGACCGGTACCCTACTCCCAAATCAAACCAAAAATATCAGGACG	47	70.4
Plasmid	pBOMB4-tet		

Primer Name	Primer Sequence (5'-3')	GC content (%)	TM (°C)
ftsK (fwd)	CGACTCCAAGTTCCTCTTCTTC	39.1	55.2
ftsK (rvs)	GATCCAGTGGTTCCTGCAATA	47.6	54.6
pbp2 (fwd)	TAACACTGACGCGGAACATAG	47.6	55.1
pbp2 (rvs)	CCGAAAGCATGAGCAGATAGA	47.6	54.8
omcB (fwd)	CGGTAGGATCTCCCTATCCTATT	47.8	54.4
omcB (rvs)	CGAACTCTGCTTCACATGGTA	47.6	55
euo (fwd)	CGAAGACTACTCGTTGGGAAATA	43.5	54.7
euo (rvs)	AACAGAAGCTCTCCTTGATAAGT	39.1	53.8

Supp. Table S2

List of primers used for RT-qPCR.

References

1. Abdelrahman Y., Ouellette Scot P., Belland Robert J., Cox John V. (2016) **Polarized Cell Division of Chlamydia Trachomatis** *PLOS Pathogens*
2. Abdelrahman Y. M., Belland R. J. (2005) **The chlamydial developmental cycle** *FEMS Microbiol Rev* **29**:949–959
3. Abdelrahman Y. O., Belland Scot P., Cox Robert J., John V. (2016) **Polarized Cell Division of Chlamydia trachomatis.** *PLOS Pathogens*
4. Barrows J. M., Goley E. D. (2021) **FtsZ dynamics in bacterial division: What, how, and why?** *Curr Opin Cell Biol* **68**:163–172
5. Bean G. J., Flickinger S. T., Westler W. M., McCully M. E., Sept D., Weibel D. B., Amann K. J. (2009) **A22 disrupts the bacterial actin cytoskeleton by directly binding and inducing a low-affinity state in MreB** *Biochemistry* **48**:4852–4857
6. Bisson-Filho A. W. *et al.* (2017) **Treadmilling by FtsZ filaments drives peptidoglycan synthesis and bacterial cell division** *Science* **355**:739–743
7. Cox J. V. A., Mohamed Yasser, Ouellette Scot P. (2020) **Penicillin-binding proteins regulate multiple steps in the polarized cell division process of Chlamydia.** *Nature*
8. Du S. L. Joe (2017) **Assembly and activation of the Escherichia coli divisome.** *Molecular Microbiology*
9. Liechti (2021) **Localized Peptidoglycan Biosynthesis in Chlamydia trachomatis Conforms to the Polarized Division and Cell Size Reduction Developmental Models.** *Front Microbiol.*
10. Kaur H., Lynn A. M. (2022) **Mapping the FtsQBL divisome components in bacterial NTD pathogens as potential drug targets** *Front Genet* **13**
11. Kemege K. E., Hickey J. M., Barta M. L., Wickstrum J., Balwalli N., Lovell S., Battaile K. P., Hefty P. S. (2015) **Chlamydia trachomatis protein CT009 is a structural and functional homolog to the key morphogenesis component RodZ and interacts with division septal plane localized MreB** *Mol Microbiol* **95**:365–382
12. Kocaoglu O., Tsui H. C., Winkler M. E., Carlson E. E. (2015) **Profiling of β -lactam selectivity for penicillin-binding proteins in Streptococcus pneumoniae D39** *Antimicrob Agents Chemother* **59**:3548–3555
13. Lee J., Cox John V., Ouellette Scot P (2020) **Critical Role for the Extended N Terminus of Chlamydial MreB in Directing Its Membrane Association and Potential Interaction with Divisome Proteins** *Journal of Bacteriology* **202**
14. Lee J. K. *et al.* (2018) **Replication-dependent size reduction precedes differentiation in Chlamydia trachomatis** *Nature Communications* **9**

15. Liechti G., Kuru E., Packiam M., Hsu Y. P., Tekkam S., Hall E., Rittichier J. T., VanNieuwenhze M., Brun Y. V., Maurelli A. T. (2016) **Pathogenic Chlamydia Lack a Classical Sacculus but Synthesize a Narrow, Mid-cell Peptidoglycan Ring, Regulated by MreB, for Cell Division** *PLoS Pathog* **12**
16. Liechti G. W., Kuru E., Hall E., Kalinda A., Brun Y. V., VanNieuwenhze M., Maurelli A. T. (2014) **A new metabolic cell-wall labelling method reveals peptidoglycan in Chlamydia trachomatis** *Nature* **506**:507–510
17. Liu X. B. Jacob, Consoli Elisa, Vollmer Waldemar, Blaauwen Tanneke den (2020) **MreC and MreD balance the interaction between the elongasome proteins PBP2 and RodA.** *PLOS Genetics*
18. Ouellette S. P., Blay E. A., Hatch N. D., Fisher-Marvin L. A. (2021) **CRISPR Interference To Inducibly Repress Gene Expression in Chlamydia trachomatis** *Infect Immun* **89**
19. Ouellette SP F.-M. L., Harpring M., Lee J, Rucks EA, Cox JV (2022) **Localized cardiolipin synthesis is required for the assembly of MreB during the polarized cell division of Chlamydia trachomatis.** *PLOS Pathogens*
20. Ouellette SP K. G., Subtil A, Ladant D. (2012) **Chlamydia co-opts the rod shape-determining proteins MreB and Pbp2 for cell division.** *Mol Microbiol.*
21. Ouellette S. P., Rueden K. J., AbdelRahman Y. M., Cox J. V., Belland R. J. (2015) **Identification and Partial Characterization of Potential FtsL and FtsQ Homologs of Chlamydia** *Front Microbiol* **6**
22. Ouellette S. P., Rueden K. J., Gauliard E., Persons L., de Boer P. A., Ladant D. (2014) **Analysis of MreB interactors in Chlamydia reveals a RodZ homolog but fails to detect an interaction with MraY** *Front Microbiol* **5**
23. Ouellette S. P. L., Junghoon Cox John V. (2020) **Division without Binary Fission: Cell Division in the FtsZ-Less Chlamydia** *Journal of Bacteriology*
24. Ouellette S. P. R., AbdelRahman Kelsey J., Cox Yasser M., Belland John V., Robert J. (2015) **Identification and Partial Characterization of Potential FtsL and FtsQ Homologs of Chlamydia.** *Frontiers in Microbiology*
25. Putman T, Hybiske K, Jow D, Afrasiabi C, Lelong S, Cano MA, Wu C, Su AI (2019) **ChlamBase: a curated model organism database for the Chlamydia research community** *Database* **2019** <https://doi.org/10.1093/database/baz041>
26. Rivas-Marín E., Canosa I., Santero E., Devos D. P. (2016) **Development of Genetic Tools for the Manipulation of the Planctomycetes** *Front Microbiol* **7**
27. Rivas-Marin E., Moyano-Palazuelo D., Henriques V., Merino E., Devos D. P. (2023) **Essential gene complement of Planctopirus limnophila from the bacterial phylum Planctomycetes** *Nat Commun* **14**
28. Stephens C (1998) **Bacterial sporulation: a question of commitment?** *Curr Biol* **8**:R45–48
29. Veiga H., Pinho M. G. (2017) **Staphylococcus aureus requires at least one FtsK/SpoIIIE protein for correct chromosome segregation** *Mol Microbiol* **103**:504–517

- 30. Wang T. J. *et al.* (2006) **Multiple biomarkers for the prediction of first major cardiovascular events and death** *N Engl J Med* **355**:2631–2639
- 31. Wang Y., Kahane S., Cutcliffe L. T., Skilton R. J., Lambden P. R., Clarke I. N. (2011) **Development of a transformation system for *Chlamydia trachomatis*: restoration of glycogen biosynthesis by acquisition of a plasmid shuttle vector** *PLoS Pathog* **7**
- 32. Wiegand S. *et al.* (2020) **Cultivation and functional characterization of 79 planctomycetes uncovers their unique biology** *Nat Microbiol* **5**:126–140
- 33. Yang X., Lyu Z., Miguel A., McQuillen R., Huang K. C., Xiao J. (2017) **GTPase activity-coupled treadmilling of the bacterial tubulin FtsZ organizes septal cell wall synthesis** *Science* **355**:744–747
- 34. Yu X. C., Tran A. H., Sun Q., Margolin W. (1998) **Localization of cell division protein FtsK to the *Escherichia coli* septum and identification of a potential N-terminal targeting domain** *J Bacteriol* **180**:1296–1304

Author information

McKenna Harpring

Department of Microbiolog, Immunology, and Biochemistry. University of Tennessee Health Science Center, Memphis, USA

Junghoon Lee

Department of Pathology, Microbiology, and Immunology, University of Nebraska Medical Center, Omaha, USA

Guangming Zhong

Department of Microbiology, Immunology, and Molecular Genetics, University of Texas Health San Antonio, San Antonio, USA

Scot P Ouellette

Department of Pathology, Microbiology, and Immunology, University of Nebraska Medical Center, Omaha, USA
ORCID iD: [0000-0002-3721-6839](https://orcid.org/0000-0002-3721-6839)

John V Cox

Department of Microbiolog, Immunology, and Biochemistry. University of Tennessee Health Science Center, Memphis, USA
ORCID iD: [0000-0002-6177-0223](https://orcid.org/0000-0002-6177-0223)

For correspondence: jcox@uthsc.edu

Editors

Reviewing Editor

Christopher Ealand

The University of the Witwatersrand, Johannesburg, South Africa

Senior Editor

Silke Hauf

Virginia Tech, Blacksburg, United States of America

Reviewer #1 (Public review):

Summary:

In this work, Harpring et al. investigated divisome assembly in *Chlamydia trachomatis* serovar L2 (Ct), an obligate intracellular bacterium that lacks FtsZ, the canonical master regulator of bacterial cell division. They find that divisome assembly is initiated by the protein FtsK in Ct by showing that it forms discrete foci at the septum and future division sites. Additionally, knocking down *ftsK* prevents divisome assembly and inhibits cell division, further supporting their hypothesis that FtsK regulates divisome assembly. Finally, they show that MreB is one of the last chlamydial divisome proteins to arrive at the site of division and is necessary for the formation of septal peptidoglycan rings but does not act as a scaffold for division assembly as previously proposed.

Strengths:

The authors use microscopy to clearly show that FtsK forms foci both at the septum as well as at the base of the progenitor cell where the next septum will form. They also show that the Ct proteins PBP2, PBP3, MreC, and MreB localize to these same sites suggesting they are involved in the divisome complex.

Using CRISPRi the authors knock down *ftsK* and find that most cells are no longer able to divide and that PBP2 and PBP3 no longer localized to sites of division suggesting that FtsK is responsible for initiating divisome assembly. They also performed a knockdown of *pbp2* using the same approach and found that this also mostly inhibited cell division. Additionally, FtsK was still able to localize in this strain, however PBP3 did not, suggesting that FtsK acts upstream of PBP2 in the divisome assembly process while PBP2 is responsible for the localization of PBP3.

The authors also find that performing a knockdown of *ftsK* also prevents new PG synthesis further supporting the idea that FtsK regulates divisome assembly. They also find that inhibiting MreB filament formation using A22 results in diffuse PG, suggesting that MreB filament formation is necessary for proper PG synthesis to drive cell division.

Overall the authors propose a new hypothesis for divisome assembly in an organism that lacks FtsZ and use a combination of microscopy and genetics to support their model that is rigorous and convincing. The finding that FtsK, rather than a cytoskeletal or "scaffolding" protein is the first division protein to localize to the incipient division site is unexpected and opens up a host of questions about its regulation. The findings will progress our understanding of how cell division is accomplished in bacteria with non-canonical cell wall structure and/or that lack FtsZ.

Weaknesses:

No major weaknesses were noted in the data supporting the main conclusions. However, there was a claim of novelty in showing that multiple divisome complexes can drive cell wall synthesis simultaneously that was not well-supported (i.e. this has been shown previously in other organisms). In addition, there were minor weaknesses in data presentation that do not substantially impact interpretation (e.g. presenting the number of cells rather than the percentage of the population when quantifying phenotypes and showing partial western blots instead of total western blots).

<https://doi.org/10.7554/eLife.104199.1.sa2>

Reviewer #2 (Public review):

Summary:

Chlamydial cell division is a peculiar event, whose mechanism was mysterious for many years. *C. trachomatis* division was shown to be polar and involve a minimal divisome machinery composed of both homologues of divisome and elongasome components, in the absence of an homologue of the classical division organizer FtsZ. In this paper, Harpring et al., show that FtsK is required at an early stage of the chlamydial divisome formation.

Strengths:

The manuscript is well-written and the results are convincing. Quantification of divisome component localization is well performed, number of replicas and number of cells assessed are sufficient to get convincing data. The use of a CRISPRi approach to knock down some divisome components is an asset and allows a mechanistic understanding of the hierarchy of divisome components.

Weaknesses:

The authors did not analyse the role of all potential chlamydial divisome components and did not show how FtsK may initiate the positioning of the divisome. Their conclusion that FtsK initiates the assembly of the divisome is an overinterpretation and is not backed by the data. However, data show convincingly that FtsK, if perhaps not the initiator of chlamydial division, is definitely an early and essential component of the chlamydial divisome.

<https://doi.org/10.7554/eLife.104199.1.sa1>

Reviewer #3 (Public review):

Summary:

The obligate intracellular bacterium *Chlamydia trachomatis* (Ct) divides by binary fission. It lacks FtsZ, but still has many other proteins that regulate the synthesis of septal peptidoglycan, including FtsW and FtsI (PBP3) as well as divisome proteins that recruit and activate them, such as FtsK and FtsQLB. Interestingly, MreB is also required for the division of Ct cells, perhaps by polymerizing to form an FtsZ-like scaffold. Here, Harpring et al. show that MreB does not act early in division and instead is recruited to a protein complex that includes FtsK and PBP2/PBP3. This indicates that Ct cell division is organized by a chimera between conserved divisome and elongasome proteins. Their work also shows convincingly that FtsK is the earliest known step of divisome activity, potentially nucleating the divisome as a single protein complex at the future division site. This is reminiscent of the activity of FtsZ, yet fundamentally different.

Strengths:

The study is very well written and presented, and the data are convincing and rigorous. The data underlying the proposed localization dependency order of the various proteins for cell division is well justified by several different approaches using small molecule inhibitors, knockdowns, and fluorescent protein fusions. The proposed dependency pathway of divisome assembly is consistent with the data and with a novel mechanism for MreB in septum synthesis in Ct.

Weaknesses:

The paper could be improved by including more information about FtsK, the "focus" of this study. For example, if FtsK really is the FtsZ-like nucleator of the Ct divisome, how is the Ct FtsK different sequence-wise or structurally from FtsK of, e.g. *E. coli*? Is the N-terminal part of FtsK sufficient for cell division in Ct like it is in *E. coli*, or is the DNA translocase also involved in focus formation or localization? Addressing those questions would put the proposed initiator role of FtsK in Ct in a better context and make the conclusions more attractive to a wider readership.

Another weakness is that the title of the paper implies that FtsK alone initiates divisome assembly. However, the data indicate only that FtsK is important at an early stage of divisome assembly, not that it is THE initiator. I suggest modifying the title to account for this--perhaps "FtsK is required to initiate....".

<https://doi.org/10.7554/eLife.104199.1.sa0>